Spin- and Gradient-Echo EPI for Imaging of Brain Perfusion with MRI

H. Schmiedeskamp[1], M. Straka[1], G. Zaharchuk[1], N. J. Fischbein[1], M. G. Lansberg[2], J-M. Olivot[2], G. W. Albers[2], M. E. Moseley[1], and R. Bammer[1]
[1]Department of Radiology, Stanford University, Stanford, CA, United States, [2]Department of Neurology, Stanford University, Stanford, CA, United States

INTRODUCTION – A spin and gradient echo (SAGE) EPI sequence that is capable of simultaneously measuring spin- (SE) and gradient-echo (GE) perfusion-weighted imaging (PWI) data was previously introduced (1). This sequence was adopted from recent work on PWI by merging multi-GE EPI (2,3) with a combined GE and SE EPI acquisition (4-6). Boxerman *et al*. (7) found a difference in sensitivity to the underlying microvasculature in brain tissue, depending on whether GE or SE images were acquired. The great advantage of SAGE-EPI is that it acquires GE and SE perfusion maps simultaneously, and allows one to relate changes in R_2 to changes in R_2* for vessel size imaging (VSI) (5,8). Here, we refined the SAGE-EPI pulse sequence to facilitate the simultaneous acquisition of 5 EPI readout trains, all with echo times TE < 100 ms. Furthermore, the PWI processing pipeline was adjusted such that cerebral blood volume (CBV) and cerebral blood flow (CBF) were calculated from R_2 and R_2* estimates, rather than relative changes in signal intensity, with the goal to produce T_1-independent, more quantitative PWI maps.

METHODS – Image acquisition was performed at 3T (gradients: 50mT/m, 200T/m/s) using 5-echo SAGE-EPI acquisition with echo times $TE_{1\text{-}5}$ = 16.6, 34.0, 61.8, 79.2, and 97.0 ms. 15 5 mm thick slices with in-plane resolution of 84x84 voxels were acquired with FOV = 24 cm. A 90° spectral-spatial RF excitation pulse was followed by a 180° spin echo refocusing pulse. Both pulses were developed using SLR design (9) with the goal of a good match between RF pulses to limit the signal drop associated with non-matched slice profiles (10). PWI was based on the subsequent acquisition of 60 EPI volumes with TR = 1800 ms. A single-dose bolus (0.1 mmol/kg body weight) of a Gadolinium-based contrast agent was administered with an MR-compatible power-injector after the onset of the dynamic image acquisition sequence (typical injection delay: 15-18 sec). Perfusion analysis was based on the calculation of R_2 and R_2* in each voxel. Perfusion parameters were obtained using the RAPID post-processing toolbox (11), which was adjusted such that the tracer concentration was derived from changes in R_2 and R_2* as follows:

$$\Delta R_2(t) = R_2(t) - R_{2,baseline} \quad and \quad \Delta R_2^*(t) = R_2^*(t) - R_{2,baseline}^* \tag{1}$$

$$S(t) = \begin{cases} S_0^I \cdot e^{-t\cdot(R_2+R_2')} & , \quad 0 < t < TE/2 \\ S_0^{II} \cdot e^{-TE\cdot R_2'} \cdot e^{-t\cdot(R_2-R_2')} & , \quad TE/2 < t \le TE. \end{cases} \tag{2}$$

R_2 and R_2* baseline estimates were calculated from pre-bolus signal averages. $R_2(t)$ and $R_2^*(t)$ were obtained through the least-squares (LSQ) solution of Eq. 2 with $R_2^* = R_2 + R_2'$. Here, $\delta = S_0^I/S_0^{II}$ was calculated during the baseline period, which was solved for the 4 parameters S_0^I, S_0^{II}, R_2, and R_2' using an LSQ approach. Thereafter, the voxel-wise estimate for δ was used as an input parameter such that the time-dependent signal eq. was solved for 3 parameters only to improve temporal stability. Relative VSI maps were extracted from the ratio of R_2- and R_2*-weighted CBV values (12). The resulting PWI maps were compared to GE PWI maps using the second echo only with TE = 34.0 ms, and with SE PWI maps (TE = 97.0 ms). VSI was compared to VSI maps calculated from the ratio between single-echo GE and SE CBV.

RESULTS – Fig. 1 shows results in case of subacute left posterior MCA infarct. While single-echo based GE and SE PWI maps reflect little to no increase in CBV (note: a 90° RF excitation pulse was used, which might have increased T_1-effects compared to lower flip angles), PWI maps produced with the help of R_2 and R_2* resulted in considerably increased CBV in the left temporal lobe (red arrows). Increased mean transit time (MTT) was associated with higher CBV, a common finding in subacute stroke lesions. VSI resulted in a small, but notable drop in vessel size within the area in question, more pronounced on the maps created with the multi-echo $\Delta R_2^*/\Delta R_2$ approach.

DISCUSSION – The incorporation of multi-echo data for the determination of the contrast agent concentration reduced T_1-shortening effects caused by leaky blood vessels (cf. Fig. 2). As seen in Fig. 3, both GE and SE based tracer concentration dropped below baseline, reducing apparent CBV and MTT. In contrast, PWI maps derived from R_2 and R_2* estimates correctly showed an increase in tracer concentration associated with leakage, thus resulted in elevated CBV and MTT, but unchanged CBF. In summary, the calculation of PWI parameters could be enhanced by correcting for T_1-shortening effects based on the estimates of the transversal relaxation times R_2 and R_2*.

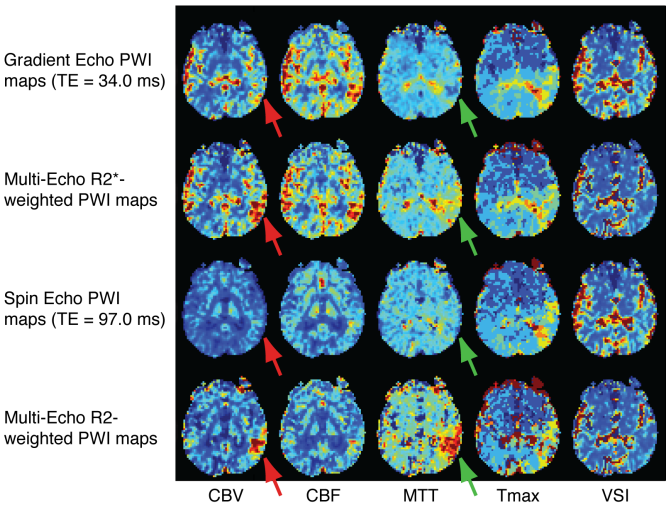

Fig. 1 *– PWI maps including CBV, CBF, MTT, Tmax, and VSI in a 76-year old patient with subacute infarct in left posterior MCA territory with enhanced CBV visible on R2 and R2*-weighted CBV maps, suppressed on single echo GE and SE CBV maps (red arrows). Associated increase in MTT, particularly well defined in R2-weighted maps. Single echo MTT maps even show a decreased MTT in questioned area (green arrows).*

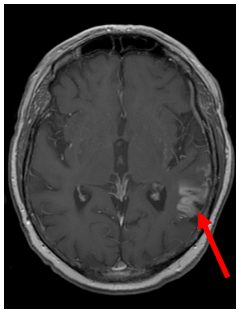

Fig. 2 *– T_1-weighted post-contrast image showing contrast agent leakage.*

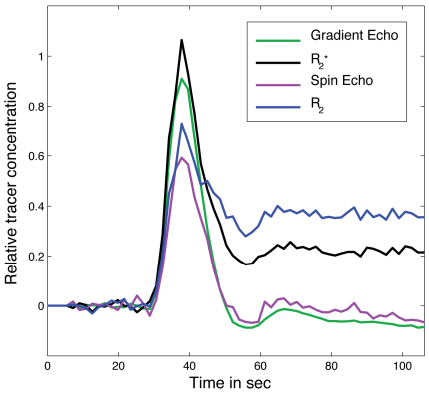

Fig. 3 *– Tracer concentration vs. time in area marked in Fig. 1. GE and SE time curves drop below baseline, resulting in apparent CBV decrease.*

REFERENCES – [1] Newbould *et al*, Proc ISMRM 2007, p1451, [2] Jochimsen *et al*, NMR Biomed 20:429-438, [3] Newbould *et al*, MRM 58:70-81, [4] Donahue *et al*, MRM 43:845-853, [5] Kiselev *et al*, MRM 53:553-563, [6] Schmainda *et al*, AJNR 25:1524-1532, [7] Boxerman *et al*, MRM 34:555-566, [8] Tropres *et al*, MRM 45:397-408, [9] Pauly *et al*, IEEE TMI 10:53-65, [10] Schmiedeskamp *et al*, Proc ISMRM 2010, p2962, [11] Straka *et al*, JMRI 32:1024-1037, [12] Schmiedeskamp *et al*, Proc ISMRM 2010, p 1785.

ACKNOWLEDGEMENTS – NIH(5R01EB002711,5R01EB008706,5R01EB006526,5R21EB006860,5R01NS047607,2P41RR009784), Lucas & Oak Foundation